

# Activated polarization pulling and de-correlation of signal and pump states of polarization in a fiber Raman amplifier

Sergey V. Sergeyev\*

Photonics Research Group, School of Engineering & Applied Science, Aston University, Birmingham, B4 7ET, UK

\*[sergey.sergeyev@gmail.com](mailto:sergey.sergeyev@gmail.com)

**Abstract:** We report on a theoretical study of activated polarization pulling and de-correlation of signal and pump states of polarization based on an advanced vector model of a fiber Raman amplifier accounting for random birefringence and two-scale fiber spinning. As a result, we have found that it is possible to provide de-correlation and simultaneously suppress PDG and PMD to 1.2 dB and  $0.035 \text{ ps/km}^{1/2}$  respectively.

©2011 Optical Society of America

**OCIS codes:** (060.2320) Fiber optics amplifiers and oscillators; (060.4370) Nonlinear optics, fibers; (190.5650) Raman effect.

---

## References and links

1. C. D. Poole and R. E. Wagner, "Phenomenological approach to polarization dispersion in long single-mode fibers," *Electron. Lett.* **22**(19), 1029–1030 (1986).
2. P. K. A. Wai and C. R. Menyuk, "Polarization mode dispersion, decorrelation and diffusion in optical fibers with randomly varying birefringence," *J. Lightwave Technol.* **14**(2), 148–157 (1996).
3. R. H. Stolen, "Polarization effects in fiber Raman and Brillouin lasers," *IEEE J. Quantum Electron.* **15**(10), 1157–1160 (1979).
4. Q. Lin and G. P. Agrawal, "Vector theory of stimulated Raman scattering and its application to fiber-based Raman amplifiers," *J. Opt. Soc. Am. B* **20**(8), 1616–1631 (2003).
5. S. Sergeyev, S. Popov, and A. T. Friberg, "Spun fiber Raman amplifiers with reduced polarization impairments," *Opt. Express* **16**(19), 14380–14389 (2008).
6. S. Sergeyev, S. Popov, and A. T. Friberg, "Virtually isotropic transmission media with fiber Raman amplifier," *IEEE J. Quantum Electron.* **46**(10), 1492–1497 (2010).
7. S. Sergeyev and S. Popov, "Two-section fiber optic Raman polarizer for high-speed transmission systems," in the 13th International Conference on Transparent Optical Networks (June 26–30, 2011) Stockholm, Sweden, Th.A6.7.
8. M. J. Li and D. A. Nolan, "Fiber spin-profile designs for producing fibers with low polarization mode dispersion," *Opt. Lett.* **23**(21), 1659–1661 (1998).
9. A. Galtarossa, L. Palmieri, A. Pizzinat, B. S. Marks, and C. R. Menyuk, "An analytical formula for the mean differential group delay of randomly-birefringent spun fibers," *J. Lightwave Technol.* **21**(7), 1635–1643 (2003).
10. M. Martinelli, M. Cirigliano, M. Ferrario, L. Marazzi, and P. Martelli, "Evidence of Raman-induced polarization pulling," *Opt. Express* **17**(2), 947–955 (2009).
11. V. V. Kozlov, J. Nuño, J. D. Ania-Castañón, and S. Wabnitz, "Theory of fiber optic Raman polarizers," *Opt. Lett.* **35**(23), 3970–3972 (2010).
12. L. Ursini, M. Santagiustina, and L. Palmieri, "Raman nonlinear polarization pulling in the pump depleted regime in randomly birefringent fibers," *IEEE Photon. Technol. Lett.* **23**(4), 254–256 (2011).
13. N. J. Muga, M. F. S. Ferreira, and A. N. Pinto, "Broadband polarization pulling using Raman amplification," *Opt. Express* **19**(19), 18707–18712 (2011).
14. J. E. Heebner, R. S. Bennink, R. W. Boyd, and R. A. Fisher, "Conversion of unpolarized light to polarized light with greater than 50% efficiency by photorefractive two-beam coupling," *Opt. Lett.* **25**(4), 257–259 (2000).
15. J. Fatome, S. Pitois, P. Morin, and G. Millot, "Observation of light-by-light polarization control and stabilization in optical fibre for telecommunication applications," *Opt. Express* **18**(15), 15311–15317 (2010).
16. A. Zadok, E. Zilka, A. Eyal, L. Thévenaz, and M. Tur, "Vector analysis of stimulated Brillouin scattering amplification in standard single-mode fibers," *Opt. Express* **16**(26), 21692–21707 (2008).
17. F. Marino, M. Giudici, S. Barland, and S. Balle, "Experimental evidence of stochastic resonance in an excitable optical system," *Phys. Rev. Lett.* **88**(4), 040601 (2002).
18. B. Lindner, J. García-Ojalvo, A. Neimand, and L. Schimansky-Geier, "Effects of noise in excitable systems," *Phys. Rep.* **392**(6), 321–424 (2004).
19. M. I. Dykman, B. Golding, L. I. McCann, V. N. Smelyanskiy, D. G. Luchinsky, R. Mannella, and P. V. E. McClintock, "Activated escape of periodically driven systems," *Chaos* **11**(3), 587–594 (2001).

20. J. D. Ania-Castañón, V. Karalekas, P. Harper, and S. K. Turitsyn, "Simultaneous spatial and spectral transparency in ultralong fiber lasers," *Phys. Rev. Lett.* **101**(12), 123903 (2008).
21. S. A. Babin, V. Karalekas, E. V. Podivilov, V. K. Mezentsev, P. Harper, J. D. Ania-Castanon, and S. K. Turitsyn, "Turbulent broadening of optical spectra in ultralong Raman fiber lasers," *Phys. Rev. A* **77**(3), 033803 (2008).

## 1. Introduction

Polarization impairments, viz. polarization mode dispersion (PMD) and polarization dependent gain (PDG), are among major factors limiting the progress in further increase of transmission rates and overall capacity of the next generation of optical networks based on distributed fiber Raman amplification. PMD leads to the pulse broadening caused by varying group velocities for the pulses with different states of polarization (SOPs) [1,2] whereas PDG leads to an uncontrollable output gain variation caused by its dependence on the input signal SOP [3–7]. By the traditional approach, spinning the fiber periodically, it is possible to reduce PMD to below 0.04 ps/km<sup>1/2</sup> [8,9], but this is accompanied with a simultaneous increase in Raman PDG [3–7]. Sergeyev *et al.* have shown that it is possible to mitigate both PDG and PMD simultaneously by using a two-section fiber ('two-section approach') in which the first section has no spin and the second one is periodically spun [5–7]. As follows from [7], this approach demonstrated polarization pulling of the signal SOP to the pump SOP and so can be considered as a two-section Raman polarizer which is the one of the techniques of all-optical polarization control [10–16]. Unlike the one-section fiber Raman polarizer demonstrated by Martinelli *et al.* [10], Kozlov *et al.* [11], L. Ursini *et al.* [12] and N. J. Muga *et al.* [13], a two-section fiber provides almost the same polarization pulling for all input signal states of polarization and so results in very small polarization dependent gain [7]. In view of increasing interest in polarization multiplexing of signals along with Raman amplification in fiber optic communication, polarization pulling approaches cannot be used straightforwardly and so have to be modified. In this paper, we have suggested a new approach based on application of fiber spinning with two different scales, viz. fast spinning with a period of 2.7 m and slow spinning with a period of more than 200 m for 10 km of single mode fiber. In view of the similarity of a two-scale periodically spun fiber Raman amplifier (SFRA) to a periodically driven excitable system (ES), we have found resonance-like de-correlation of pump and signal SOPs and polarization pulling equivalent to the Stochastic Resonance (SR) and Dynamic Localization (DL) in ES [17–19]. As a result, we have demonstrated that it is possible to provide de-correlation of pump and signal SOPs and simultaneously suppress PDG and PMD to the 1.2 dB and 0.035 ps/km<sup>1/2</sup> respectively. The practical implementation of the obtained results can be in the design of a fiber Raman amplifier-based quasi-isotropic spatially and spectrally transparent media for high-speed fiber optic communication [20,21].

## 2. Model of a fiber Raman amplifier with random birefringence and arbitrary spin profile

The evolution of signal and pump states of polarization in a single mode fiber is typically described in terms of the unit vectors  $\hat{\mathbf{s}} = (\hat{s}_1, \hat{s}_2, \hat{s}_3)$  and  $\hat{\mathbf{p}} = (\hat{p}_1, \hat{p}_2, \hat{p}_3)$ , respectively, pointing to positions on the Poincaré sphere (Fig. 1). Due to birefringence, these vectors rotate on the Poincaré sphere around the birefringence vector  $\mathbf{W}_i = (2b_i \cos \theta, 2b_i \sin \theta, 0)^T$  in the same direction, but at different rates  $b_s$  and  $b_p$  which are birefringence strengths ( $b_i = \pi/L_{bi}$  where  $L_{bi}$  is the beat length) at signal  $\lambda_s$  and pump  $\lambda_p$  wavelengths. We assume that the birefringence strength  $2b_i$  is fixed and the orientation angle  $\theta$  is driven by a white-noise process (fixed-modulus model [2])

$$\frac{d\theta}{dz} = \beta(z), \langle \beta(z) \rangle = 0, \langle \beta(z) \beta(z') \rangle = \sigma^2 \delta(z - z'), \quad (1)$$

where  $\langle \dots \rangle$  means averaging over the birefringence fluctuations along the fiber,  $\delta(z)$  is a Dirac delta-function, and  $\sigma^2 = 2/L_c$  ( $L_c$  is the birefringence correlation length).

We neglect herein the fiber twist and, therefore, the birefringence vector for the spun fiber takes the form of  $\mathbf{W}_i = R_3[2A(z)]\mathbf{W}_{i,un}$ , where  $A(z)$  is the spin profile, and  $R_3(\gamma)$  represents rotation in the equatorial plane by angle  $\gamma$  around the  $z$ -axis on the Poincaré sphere [9]

$$R_3(\gamma) = \begin{bmatrix} \cos \gamma & -\sin \gamma & 0 \\ \sin \gamma & \cos \gamma & 0 \\ 0 & 0 & 1 \end{bmatrix}. \quad (2)$$

Stimulated Raman scattering leads to amplification of the signal wave and changes its direction and so evolution of the signal  $\mathbf{S}$  and pump  $\mathbf{P}$  SOPs can be found as follows:

$$\mathbf{S} = s_0 G_{ave} \hat{\mathbf{s}}, \quad \mathbf{P} = P_0(z) \hat{\mathbf{p}}. \quad (3)$$

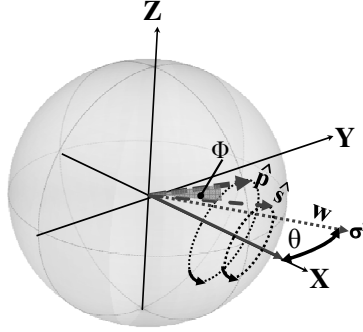


Fig. 1. Evolution of the pump  $\hat{\mathbf{p}}$  and the signal  $\hat{\mathbf{s}}$  states of polarization on the Poincaré sphere, as well as the fluctuations of the local birefringence vector  $\mathbf{W}_i = (2b_i \cos \theta, 2b_i \sin \theta, 0)^T$ . Vectors  $\hat{\mathbf{s}}$  and  $\hat{\mathbf{p}}$  rotate around the local axis ( $\mathbf{W}$ ) at rates  $b_p$  and  $b_s$ , while vector ( $\mathbf{W}$ ) rotates randomly in the equatorial plane at the rate  $\sigma = L_c^{-1/2}$  ( $L_c$  is the correlation length),  $\Phi$  is an angle between pump and signal SOPs.

Here  $s_0$  is the part of the signal amplitude related to the pump-signal SOPs interaction,

$$G_{ave} = \exp \left( \int_0^z g P_0(z') / 2 dz' - \alpha_s z \right)$$
 is the averaged Raman gain,  $g$  is the Raman gain

coefficient, the forward pump power  $P_0(z) = P_{in} \exp(-\alpha_p z)$ ;  $\alpha_s$  and  $\alpha_p$  are the signal and pump losses, respectively;  $L$  is the fiber length. The part of the Raman gain  $\Delta G$  related to polarization evolution due to random birefringence and fiber spinning depends on  $s_0$  as follows [4–7]:

$$\Delta G \equiv 10 \log \left( \frac{\langle S_0(L) \rangle}{\langle S_0(0) \rangle} / G_{ave} \right) = 10 \log \left( \frac{\langle s_0(L) \rangle}{\langle s_0(0) \rangle} \right), \quad (4)$$

where  $\langle \dots \rangle$  means averaging over the birefringence fluctuations along the fiber. If the input pump and signal SOPs are parallel Raman gain takes the maximum value and if the SOPs are orthogonal than Raman gain takes the minimum one [4–7]. The difference in gains (polarization dependent gain, PDG) can be found as follows [4–7]

$$PDG \equiv 10 \log \left( \langle s_{0,max}(L) \rangle / \langle s_{0,min}(L) \rangle \right), \quad (5)$$

To characterize de-correlation of pump and signal SOPs and polarization pulling in terms of the Stochastic Resonance phenomenon we introduce parameter  $R$  which is similar to the signal-to-noise ratio in the models of SR [18]:

$$R = -5 \log \left( \frac{\langle s_{0,\max(\min)}^2(L) \rangle - \langle s_{0,\max(\min)}(L) \rangle^2}{\langle s_{0,\max(\min)}(L) \rangle^2} \right). \quad (6)$$

To calculate  $s_0(L)$ , we use a vector model of a fiber Raman amplifier for forward pump with allowance for fiber spin profile and random birefringence and neglecting pump depletion [4]:

$$\begin{aligned} \frac{d\mathbf{s}}{dz} &= \frac{g}{2} P_0(z) s_0 \hat{\mathbf{p}} + (\mathbf{W}_s + \mathbf{W}_s^{(NL)}) \times \mathbf{s}, \\ \frac{d\hat{\mathbf{p}}}{dz} &= (\mathbf{W}_p + \mathbf{W}_p^{(NL)}) \times \hat{\mathbf{p}}. \end{aligned} \quad (7)$$

Here  $\mathbf{s} = s_0 \hat{\mathbf{s}}$ , and  $\mathbf{W}_p^{(NL)}$ ,  $\mathbf{W}_s^{(NL)}$  describes the nonlinear SOP evolution caused by self- and cross-phase modulation (SPM and XPM):  $\mathbf{W}_p^{(NL)} = 2\gamma_p/3(-2S_1, -2S_2, \hat{p}_3 P_0(z))$ ,  $\mathbf{W}_s^{(NL)} = 2\gamma_s/3(-2\hat{p}_1 P_0(z), -2\hat{p}_2 P_0(z), S_3)$ . Kerr coupling constants are  $\gamma_i = 2\pi n_2/(\lambda_i A_{eff})$  ( $i = s, p$ ), where  $n_2$  is the nonlinear Kerr coefficient and  $A_{eff}$  is the effective core area of the fiber.

We choose the reference frame in the Stokes space in such a way that the local birefringence vector is  $\tilde{\mathbf{W}}_{i,un} = (2b_i, 0, 0)$  and  $\hat{\mathbf{p}}(0) = (1, 0, 0)$ , i.e. oriented along the  $X$ -axis on the Poincaré sphere. This can be accomplished by a suitable transformation  $\tilde{\mathbf{W}}_i = \mathbf{R}_3^{-1}(\theta + 2A(z)) \mathbf{W}_i$ , and  $\tilde{\mathbf{s}} = \mathbf{R}_3^{-1}(\theta + 2A(z)) \mathbf{s}$  and  $\hat{\mathbf{p}} = \mathbf{R}_3^{-1}(\theta + 2A(z)) \hat{\mathbf{p}}$ , provided the variable  $s_0$  and scalar product  $x = \hat{\mathbf{p}} \cdot \mathbf{s}$  are invariant under the rotation. In addition, we consider cases which correspond to the maximum and minimum of Raman gain, viz.  $\tilde{\mathbf{s}}_{\max}(0) = (1, 0, 0)$  and  $\tilde{\mathbf{s}}_{\min}(0) = (-1, 0, 0)$ . Applying an averaging procedure considered in [5,6] to Eqs. (7), we find the system of equations:

$$\begin{aligned} \frac{d\langle s_0 \rangle}{dz'} &= \varepsilon_1 \exp(-\varepsilon_2 z') \langle x \rangle, \\ \frac{d\langle x \rangle}{dz'} &= \varepsilon_1 \exp(-\varepsilon_2 z') \langle s_0 \rangle - \varepsilon_3 \langle y \rangle - (\delta_p - \delta_s) \exp(-\varepsilon_2 z') \langle \hat{p}_3 (\hat{p}_2 \tilde{s}_1 - \hat{p}_1 \tilde{s}_2) \rangle, \\ \frac{d\langle y \rangle}{dz'} &= \varepsilon_3 \left[ \langle x \rangle - \langle \hat{p}_1 \tilde{s}_1 \rangle \right] - 2\alpha(z') \langle u \rangle - \frac{\langle y \rangle L}{2L_c} + \varepsilon_4 \langle \hat{p}_2 \tilde{s}_1 \rangle - \varepsilon_5 \langle \hat{p}_1 \tilde{s}_2 \rangle - \\ &(\delta_p - \delta_s) \exp(-\varepsilon_2 z') \langle \hat{p}_3 \hat{p}_1 \tilde{s}_3 \rangle - \delta_s \exp(-\varepsilon_2 z') \langle \hat{p}_2 (\hat{p}_2 \tilde{s}_1 - \hat{p}_1 \tilde{s}_2) \rangle, \\ \frac{d\langle u \rangle}{dz'} &= 2\alpha(z') \langle y \rangle - \frac{\langle u \rangle}{2} + (\delta_p - \delta_s) \exp(-\varepsilon_2 z') \langle \hat{p}_3 \hat{p}_2 \tilde{s}_3 \rangle - \delta_s \exp(-\varepsilon_2 z') \langle \hat{p}_1 (\hat{p}_2 \tilde{s}_1 - \hat{p}_1 \tilde{s}_2) \rangle. \end{aligned} \quad (8)$$

Here  $\delta_p = 2\gamma_p LP_{in}/3$ ,  $\delta_s = 4\gamma_s LP_{in}/3$ ,  $\langle x \rangle = \langle \hat{p}_1 \tilde{s}_1 + \hat{p}_2 \tilde{s}_2 + \hat{p}_3 \tilde{s}_3 \rangle$ ,  $\langle y \rangle = \langle \hat{p}_3 \tilde{s}_2 - \hat{p}_2 \tilde{s}_3 \rangle$ ,  $\langle u \rangle = \langle \hat{p}_3 \tilde{s}_1 - \hat{p}_1 \tilde{s}_3 \rangle$ ,  $\alpha(z') = \partial A(z')/\partial z'$  is the spin rate,  $z' = z/L$ ,  $\varepsilon_1 = g P_{in} L/2$ ,  $\varepsilon_2 = \alpha_s L$ ,  $\varepsilon_3 = 2\pi L/L_{bp} (\lambda_s/\lambda_p - 1)$ ,  $\varepsilon_4 = (2\pi L)/L_{bp}$ ,  $\varepsilon_5 = (2\pi L)/L_{bs}$ .

In view of  $\varepsilon_3 \ll \varepsilon_4$ ,  $\varepsilon_5$  (rotation of the signal SOP with respect to the pump SOP is much slower than the SOPs rotation with respect the local birefringence vector  $\tilde{\mathbf{W}}_i$ ), we can average over the fast rotations. It can be done by the transformations  $h = \mathbf{R}_s(z) \tilde{\mathbf{s}}$  and  $f = \mathbf{R}_p(z) \hat{\mathbf{p}}$ , where

$$\mathbf{R}_i(z) = \begin{pmatrix} 1 & 0 & 0 \\ 0 & \cos(2b_i z) & \sin(2b_i z) \\ 0 & -\sin(2b_i z) & \cos(2b_i z) \end{pmatrix}, \quad (i = s, p). \quad (9)$$

Using this transformation, Eq. (7) and averaging over the fast oscillations, we find the following equation for  $\langle h_1 f_1 \rangle$

$$\frac{d\langle h_1 f_1 \rangle}{dz'} = \varepsilon_1 \exp(-\varepsilon_2 z') \langle s_0 f_1^2 \rangle - \frac{L}{L_c} \langle h_1 f_1 \rangle. \quad (10)$$

If we choose parameters for Raman amplifier as,  $g = 2.3 \text{ dB W}^{-1} \text{ km}^{-1}$ ,  $P_{in} = 5 \text{ W}$ ,  $L = 10 \text{ km}$ ,  $L_c = 110 \text{ m}$ , we find that  $\varepsilon_1 L_c / L = 0.15 \ll 1$ . Thus, we can neglect the first term on the right-hand side of Eq. (10). As a result,

$$\langle \hat{p}_1 \tilde{s}_1 \rangle = \langle h_1 f_1 \rangle = \hat{p}_1(0) \tilde{s}_1(0) \exp(-z' L / L_c). \quad (11)$$

In addition, this procedure leads to  $\langle \hat{p}_2 \tilde{s}_1 \rangle \rightarrow 0$ ,  $\langle \hat{p}_1 \tilde{s}_2 \rangle \rightarrow 0$ ,  $\langle \hat{p}_2 \hat{p}_3 \tilde{s}_2 \rangle \rightarrow 0$ ,  $\langle \hat{p}_1 \hat{p}_3 \tilde{s}_2 \rangle \rightarrow 0$ ,

$\langle \hat{p}_3 (\hat{p}_2 \tilde{s}_1 - \hat{p}_1 \tilde{s}_2) \rangle \rightarrow 0$  and so self- and cross-phase modulation (SPM and XPM) can be neglected [4–7]. A similar result has been obtained in [10,12] by direct modeling of stochastic Eqs. (7), viz. it was obtained that for the pump power  $P_{in} < 10 \text{ W}$  and PMD parameter  $D_p > 0.01 \text{ ps/km}^{1/2}$  SPM and XPM has no contribution to polarization pulling. Using transformation (9) and averaging over the birefringence fluctuations and fast oscillations we find the following equations which we use to calculate parameter R from Eq. (6):

$$\begin{aligned} \frac{d\langle s_0^2 \rangle}{dz'} &= 2\varepsilon_1 \exp(-\varepsilon_2 z') \langle s_0 x \rangle, \\ \frac{d\langle s_0 x \rangle}{dz'} &= \varepsilon_1 \exp(-\varepsilon_2 z') (\langle s_0^2 + x^2 \rangle) - \varepsilon_3 \langle y s_0 \rangle, \\ \frac{d\langle s_0 y \rangle}{dz'} &= \varepsilon_1 \exp(-\varepsilon_2 z') \langle xy \rangle + \varepsilon_3 [\langle s_0 x \rangle - \langle y^2 \rangle - \langle s_0 \rangle \langle \hat{p}_1 \tilde{s}_1 \rangle] - 2\alpha(z') \langle s_0 u \rangle - \frac{\langle s_0 y \rangle L}{2L_c}, \\ \frac{d\langle x^2 \rangle}{dz'} &= 2\varepsilon_1 \exp(-\varepsilon_2 z') \langle s_0 x \rangle - 2\varepsilon_3 \langle xy \rangle, \\ \frac{d\langle xy \rangle}{dz'} &= \varepsilon_1 \exp(-\varepsilon_2 z') \langle s_0 y \rangle + \varepsilon_3 [\langle x^2 \rangle - \langle x \rangle \langle \hat{p}_1 \tilde{s}_1 \rangle] - 2\alpha(z') \langle xu \rangle - \frac{\langle xy \rangle L}{2L_c}, \\ \frac{d\langle u s_0 \rangle}{dz'} &= \varepsilon_1 \exp(-\varepsilon_2 z') \langle xu \rangle + 2\alpha(z') \langle y s_0 \rangle - \frac{\langle u s_0 \rangle L}{2L_c}, \\ \frac{d\langle xu \rangle}{dz'} &= \varepsilon_1 \exp(-\varepsilon_2 z') \langle s_0 u \rangle - \varepsilon_3 \langle yu \rangle + 2\alpha(z') \langle xy \rangle - \frac{\langle xu \rangle L}{2L_c}, \\ \frac{d\langle yu \rangle}{dz'} &= \varepsilon_3 (\langle xu \rangle - \langle u \rangle \langle \hat{p}_1 \tilde{s}_1 \rangle) + 2\alpha(z') (\langle y^2 \rangle - \langle u^2 \rangle) + \frac{L \langle yu \rangle}{2L_c}, \\ \frac{d\langle u^2 \rangle}{dz'} &= 2\alpha(z') \langle yu \rangle + \frac{L}{L_c} (\langle y^2 \rangle - \langle u^2 \rangle), \\ \frac{d\langle y^2 \rangle}{dz'} &= 2\varepsilon_3 [\langle yx \rangle - \langle y \rangle \langle \hat{p}_1 \tilde{s}_1 \rangle] - 2\alpha(z') \langle yu \rangle - \frac{L}{L_c} (\langle y^2 \rangle - \langle u^2 \rangle). \end{aligned} \quad (12)$$

To calculate the spin induced reduction factor (SIRF) for the case of spun fiber we use the standard model of PMD [9]

$$\frac{d\mathbf{\Omega}}{dz} = \frac{\partial \mathbf{W}_s}{\partial \omega} + \mathbf{W}_s \times \mathbf{\Omega}, \quad SIRF = \sqrt{\left\langle |\mathbf{\Omega}(L)|_{sp}^2 \right\rangle / \left\langle |\mathbf{\Omega}(L)|_{un}^2 \right\rangle}, \quad (13)$$

where  $\left\langle |\mathbf{\Omega}(L)|_{sp}^2 \right\rangle$  and  $\left\langle |\mathbf{\Omega}(L)|_{un}^2 \right\rangle$  are the mean-square differential group delays (DGD) for two orthogonal SOPs in the case of long-length spun fiber and the same fiber without spin, respectively [9]. As follows from [5,6,9], after averaging over fluctuations caused by random birefringence, equations for SIRF take the following form:

$$\begin{aligned} \frac{d SIRF^2}{dz'} &= \langle \hat{\Omega}_1 \rangle, \\ \frac{d \langle \hat{\Omega}_1 \rangle}{dz'} &= -\langle \hat{\Omega}_1 \rangle L/L_c + 2\alpha(z) \langle \hat{\Omega}_2 \rangle + L/L_c, \\ \frac{d \langle \hat{\Omega}_2 \rangle}{dz'} &= -2\alpha(z) \langle \hat{\Omega}_1 \rangle - \langle \hat{\Omega}_2 \rangle L/L_c - \varepsilon_5 \langle \hat{\Omega}_3 \rangle, \\ \frac{d \langle \hat{\Omega}_3 \rangle}{dz'} &= \varepsilon_5 \langle \hat{\Omega}_2 \rangle. \end{aligned} \quad (14)$$

Finally, the PMD parameter for the spun fiber  $D_{ps}$  can be found as follows [9]

$$D_{ps} = \frac{\lambda_s \sqrt{2L_c}}{L_{bs} c} SIRF. \quad (15)$$

In addition, we use fast periodic spinning along with slow- amplitude and phase modulation:

$$\begin{aligned} \alpha_{am}(z') &= A_0 k_{hf} L \cos(k_{lf} L z') \cos(k_{hf} L z'), \\ \alpha_{pm}(z') &= A_0 k_{hf} L \cos\left(k_{hf} \left(L z' + a_0 \cos(k_{lf} L z')\right)\right). \end{aligned} \quad (16)$$

Here  $A_0$  is amplitude of the fiber spinning in rad,  $k_{lf}$  and  $k_{hf}$  are low and high frequencies of the fiber spinning. Practical realization of amplitude- and phase-modulated fiber spinning can be achieved based on the modern technology of direct fiber spinning instead of spinning the preform [8].

To quantify polarization pulling and SOPs de-correlation in terms of SR phenomena, we calculate parameters equivalent to the parameters used in the models of excitable systems [17–19], viz. Kramers length  $\langle L_k \rangle$  and intrawell relaxation length  $\langle L_R \rangle$ . In the absence of low-frequency modulation ( $k_{lf} = 0$ ), Eqs. (8) can be simplified for the case of  $k_{hf} \gg L_c$ ,  $L_b$  with the help of averaging over fast periodic fiber spinning [9]. As a result, we have

$$\begin{aligned} \frac{d \langle \hat{x} \rangle}{dz'} &= \varepsilon_1 \exp(-\varepsilon_2 z') (1 - \langle \hat{x} \rangle^2) - \varepsilon_3 \langle \hat{y} \rangle, \\ \frac{d \langle \hat{y} \rangle}{dz'} &= \left( J_0(2A_0)^2 \varepsilon_3 - \varepsilon_1 \exp(-\varepsilon_2 z') \langle \hat{y} \rangle \right) \langle \hat{x} \rangle - \frac{\langle \hat{y} \rangle L}{2L_c}. \end{aligned} \quad (17)$$

Here  $\langle \hat{y} \rangle = \langle y \rangle / \langle s_0 \rangle$ ,  $\langle \hat{x} \rangle \equiv \cos \Phi = \langle x \rangle / \langle s_0 \rangle$  is the variable which indicates polarization pulling if  $\langle \hat{x} \rangle \rightarrow 1$  or de-correlation pump and signal SOPs if  $\langle \hat{x} \rangle \rightarrow 0$ ; and  $J_0(2A_0)$  is the zero-order Bessel function of the first kind. For  $\exp(-\varepsilon_2 z') \ll 1$ , solutions of Eqs. (17)  $\langle \hat{x}_0 \rangle, \langle \hat{y}_0 \rangle$  independent on  $z'$ , can be found from equations:

$$\Delta^2 \langle \hat{x}_0 \rangle^3 + \Delta \langle \hat{x}_0 \rangle^2 + (\Delta_1^2 - \Delta^2) \langle \hat{x}_0 \rangle - \Delta = 0, \quad (18)$$

$$\langle \hat{y}_0 \rangle = \frac{J_0(2A_0)\Delta_1 \langle \hat{x}_0 \rangle}{\Delta \langle \hat{x}_0 \rangle + 1}.$$

Here  $\Delta = 2L_c \varepsilon_1 \exp(-\varepsilon_2 z')/L$ ,  $\Delta_1 = 2L_c J_0(2A_0) \varepsilon_3/L$ . Linear stability analysis of Eqs. (17) near the states  $\langle \hat{x}_0 \rangle, \langle \hat{y}_0 \rangle$  results in the following eigenvalues:

$$\Lambda_{1,2} = -\frac{1}{4L_c}(3\Delta \langle \hat{x}_0 \rangle + 1) \pm \frac{1}{4L_c} \sqrt{1 + \Delta^2 \langle \hat{x}_0 \rangle^2 - 2\Delta \langle \hat{x}_0 \rangle - 4\Delta_1^2 + \Delta \Delta_1 \langle \hat{y}_0 \rangle}. \quad (19)$$

Thus, relaxation length can be defined as  $\langle L_R \rangle = 1/\text{Re}(\Lambda_{1,2})$ . If  $\text{Im}(\Lambda_{1,2}) \neq 0$  then the system oscillates around the states  $\langle \hat{x}_0 \rangle, \langle \hat{y}_0 \rangle$  and so the averaged length at which the system is close to the state can be defined as  $\langle L_k \rangle = 2\pi L/\text{Im}(\Lambda_{1,2})$  (Kramers length).

### 3. Results and discussion

We have found  $\langle \hat{x}_0 \rangle, \langle \hat{y}_0 \rangle, \text{Re}\{\Lambda_{1,2}\}, \text{Im}\{\Lambda_{1,2}\}$  numerically from Eqs. (18), (19). We find also PDG, R and PMD parameter  $D_p$  numerically from Eqs. (5), (6), (8) and (12)–(15) for two-scale fiber spinning (16). We use parameters typical for a distributed fiber Raman amplifier:  $L = 10 \text{ km}$ ,  $\alpha_s = 0.2 \text{ dB/km}$ ,  $\lambda_p = 1460 \text{ nm}$ ,  $\lambda_s = 1550 \text{ nm}$ ,  $g = 2.3 \text{ dBW}^{-1}\text{km}^{-1}$ ,  $P_{in} = 5 \text{ W}$ ,  $L_b = 8.3 \text{ m}$ ,  $A_0 = 3$  (in units of  $\text{rad}$ ),  $k_{hf} = 6\pi/L_{bp}$ ,  $k_{lf} = [0 \dots 300/L]$ ,  $L_c = [5 \text{ m} \dots 205 \text{ m}]$ ,  $a_0 = 100 \text{ m}$ . Results for  $\langle \hat{x}_0 \rangle, \langle \hat{y}_0 \rangle$  and  $\text{Re}\{\Lambda_1\}, \text{Im}\{\Lambda_1\}$  are shown in Fig. 2 (a, b). The results for PDG, R and PMD parameters with  $\hat{\mathbf{p}}(0) = (1, 0, 0)$ ,  $\hat{\mathbf{s}}_{\min}(0) = (-1, 0, 0)$ ,  $\hat{\mathbf{s}}_{\max}(0) = (1, 0, 0)$  are shown in Fig. 3 (a-f).

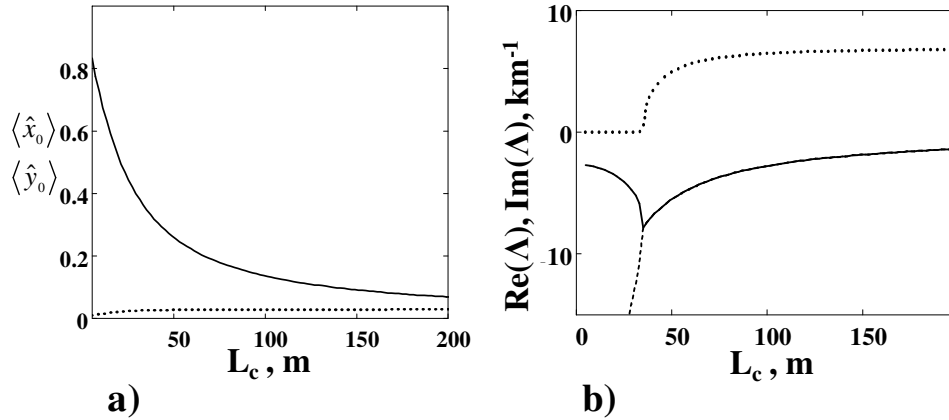


Fig. 2. a):  $\langle \hat{x}_0 \rangle$  (solid line) and  $\langle \hat{y}_0 \rangle$  (dotted line) and b):  $\text{Im}(\Lambda_1), \text{Im}(\Lambda_2)$ , (dotted line),  $\text{Re}(\Lambda_1)$  (solid line) and  $\text{Re}(\Lambda_2)$  (dashed line) as a function of correlation length  $L_c$ .

Parameters:  $L = 10 \text{ km}$ ,  $\alpha_s = 0.2 \text{ dB/km}$ ,  $\lambda_p = 1460 \text{ nm}$ ,  $\lambda_s = 1550 \text{ nm}$ ,  $g = 2.3 \text{ dBW}^{-1}\text{km}^{-1}$ ,  $P_{in} = 5 \text{ W}$ ,  $L_b = 8.3 \text{ m}$ ,  $A_0 = 3$  (in units of  $\text{rad}$ ),  $k_{hf} = 6\pi/L_{bp}$ ,  $k_{lf} = 0$ ,  $L_c = [5 \text{ m} \dots 205 \text{ m}]$ .

For the parameters listed, Eqs. (18) have only one real solution with  $|\langle \hat{x}_0 \rangle| \leq 1$ . As follows from Fig. 2 (a) for  $L_c \rightarrow 0$  (high birefringence fluctuations)  $\langle \hat{x}_0 \rangle \rightarrow 1$  and so we have

polarization pulling and for  $L_c \gg 200 \text{ m}$  de-correlation of SOPs with  $\langle \hat{x}_0 \rangle \rightarrow 0$ . It is clear from Fig. 2 (b) that oscillations of angle between SOPs start when  $L_c \geq 35 \text{ m}$ .

As a result of nonlinearity in the form of Raman amplification and presence of random birefringence and periodic fiber spinning, *PDG* has maxima and minima as a function of correlation length  $L_c$  and spinning frequency  $k_{lf}$ . For slow amplitude modulation of the fiber spinning (Fig. 3 (a)), the maximum *PDG* corresponds to the case when  $L_c, k_{lf} \rightarrow 0$ . As follows from the results of [8,9], fast periodic fiber spinning results in PMD mitigation and so leads to polarization pulling [7–13]. However, with increased frequency of amplitude modulation *PDG* reaches a minimum of 1.5 dB for  $L_c = 105 \text{ m}$  and  $k_{lf} = 6 \text{ km}^{-1}$  and for  $L_c = 55 \text{ m}$  and  $k_{lf} = 30 \text{ km}^{-1}$  *PDG* reaches the maximum of 6.9 dB (Fig. 3 (a)). In the case of slow phase modulation, *PDG* reaches a minimum of 1.2 dB for  $L_c = 110 \text{ m}$  and  $k_{lf} = 3 \text{ km}^{-1}$  and a maximum of 14.5 dB for  $L_c = 110 \text{ m}$  and  $k_{lf} = 22 \text{ km}^{-1}$  (Fig. 3 (b)).

The evolution of angle  $\Phi$  between pump and signal SOPs for the cases of minima and maxima is shown in Figs. 4. As follows from Figs. 3 (a, b) and Figs. 4, the maximum of *PDG* corresponds to the polarization pulling with  $\cos \Phi \rightarrow 1$ , and the minimum of *PDG* corresponds to the case of SOPs de-correlation for which pump and signal SOPs are freely rotating and so  $\cos \Phi \rightarrow 0$ . In addition, fiber spinning with low-frequency phase modulation provides better polarization pulling as compared to the case of amplitude modulation (thick lines in Figs. 4).

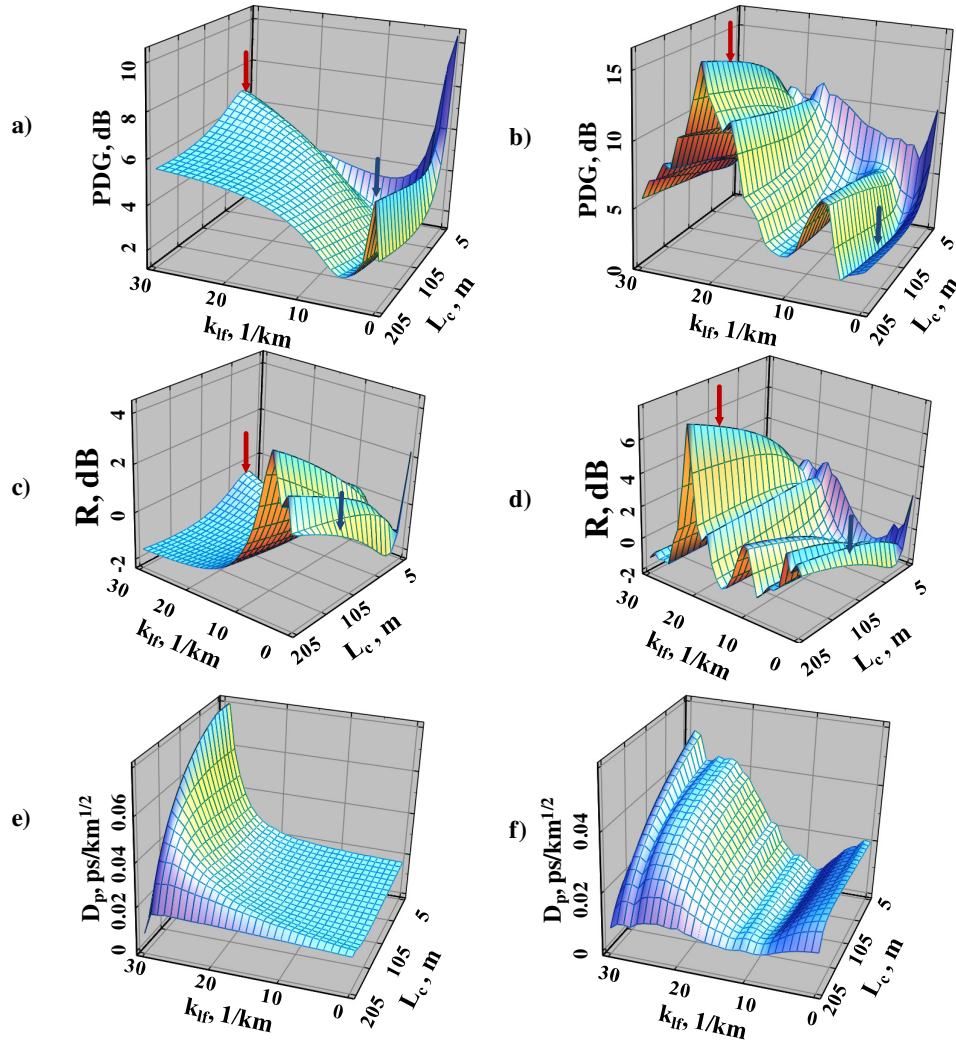


Fig. 3. Polarization dependent gain  $PDG$  (a, b), parameter  $R$  for the  $\hat{\mathbf{p}}(0) = \hat{\mathbf{s}}_{\max}(0) = (1, 0, 0)$  (c, d) and PMD parameter  $D_p$  (e, f) as a function of fiber spinning frequency  $k_{lf}$  and correlation length  $L_c$ . Low-frequency amplitude (a, c, e) and phase modulated (b, d, f) fiber spinning. Parameters are the same as for Fig. 2. De-correlation of pump and signal SOPs (minimum in  $PDG$  with an arrow):  $L_c = 105$  m and  $k_{lf} = 6$   $km^{-1}$  (Figs. 3 (a, c)),  $L_c = 110$  m and  $k_{lf} = 3$   $km^{-1}$  (Figs. 3 (b, d)); polarization pulling (maximum in  $PDG$  with an arrow):  $L_c = 35$  m and  $k_{lf} = 30$   $km^{-1}$  (Figs. 3 (a, c)),  $L_c = 110$  m and  $k_{lf} = 22$   $km^{-1}$  (Figs. 3 (b, d)).

To characterize polarization pulling and SOPs de-correlation in terms of SR phenomena, we present in Fig. 5 (a-d) the results for  $PDG$ , parameter  $R$  and PMD parameter  $D_p$  as a function of modulation frequency  $k_{lf}$  and correlation length  $L_c$ . For low-frequency amplitude modulation,  $PDG$  has a minimum and parameter  $R$  has a maximum at frequency of  $k_{lf,max} = 6$   $km^{-1}$  which coincides with the resonance frequency for excitable systems calculated from Eq. (19).

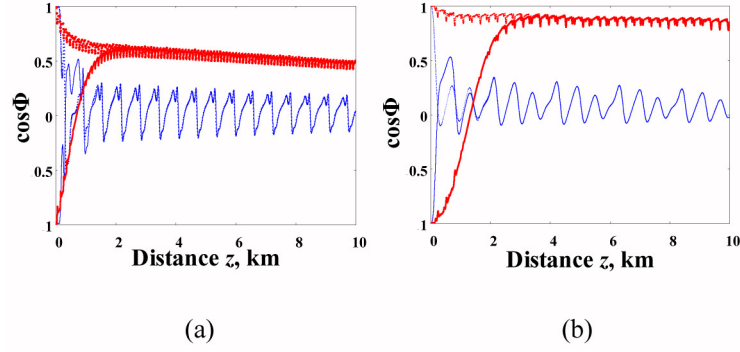


Fig. 4. Polarization pulling metrics  $\cos\Phi$  as a function of distance along the fiber  $z$  for low-frequency amplitude (a) and phase modulated (b) fiber spinning. Dotted line:  $\tilde{s}_{\max}(0) = (1, 0, 0)$ , solid line  $\tilde{s}_{\min}(0) = (-1, 0, 0)$ . Thick lines and thin lines correspond to the maximum and minimum in PDG shown by arrows.

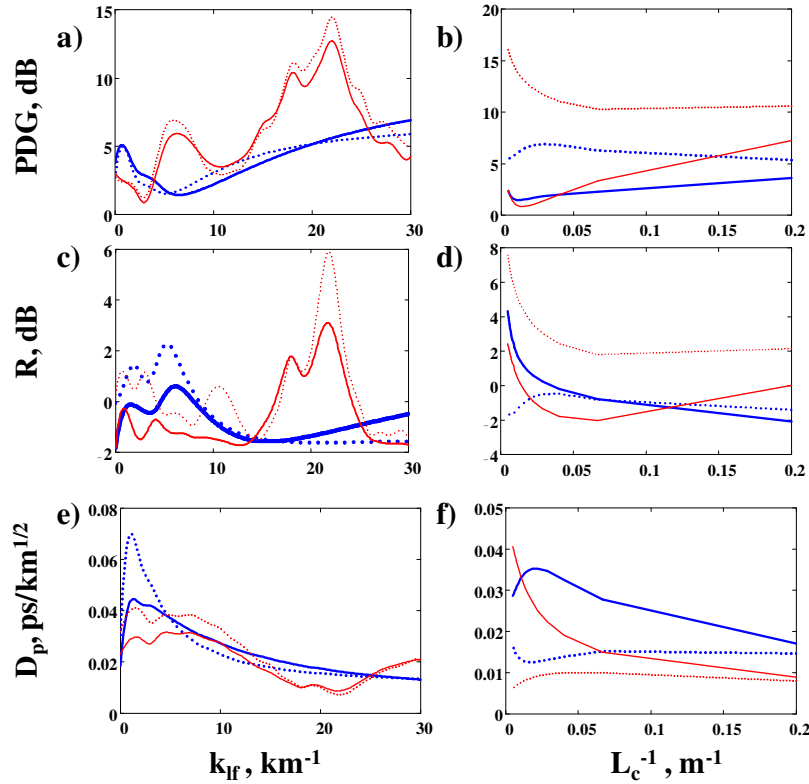


Fig. 5. PDG (a,b), parameter  $R$  (c, d) and PMD parameter  $D_p$  (e, f) as a function of modulation frequency  $k_{lf}$  (a, c) and correlation length  $L_c$  (b, d) for amplitude (thick lines) and phase modulated (thin lines) of fiber spinning. Parameters in Figs. 5 (a, c, d):  $L_c = 35$  m (thick solid line),  $L_c = 105$  m (thick dotted line),  $L_c = 55$  m (thin solid line),  $L_c = 115$  m (thin dotted line), Parameters in Figs. 5 (b, d, f):  $k_{lf} = 6$   $\text{km}^{-1}$  (thick solid line),  $k_{lf} = 30$   $\text{km}^{-1}$  (thick dotted line),  $k_{lf} = 3$   $\text{km}^{-1}$  (thin solid line),  $k_{lf} = 22$   $\text{km}^{-1}$  (thin dotted line).

A maximum and minimum at this frequency is evidence of Stochastic Resonance where random birefringence fluctuations are synchronized with an external modulation [18]. In view of the maximum in  $R$  coinciding with the minimum in  $PDG$ , SR for this case corresponds to

de-correlation of the pump and input SOPs. For the off-resonance conditions (low and high frequencies of spinning), the random birefringence fluctuations have no synchronization with the external modulation and so there is no activation of de-correlation of pump and signal SOPs. For the case of phase modulated fiber spinning, PDG and parameter  $R$  have maxima and minima at frequencies different from SR frequencies (thin lines in Figs. 5 (a, c)). It is quite similar to the case of Dynamic Localization (DL) considered by Dykman *et al.*, where the right and the left escape rates become different to each other depending on the phase of non-adiabatic aperiodic modulation [19]. Thus, DL phenomena take the form of either polarization pulling or de-correlated SOPs depending on the phase of phase modulated fiber spinning. It is likely that increased noise power  $\sigma^2$  ( $\sigma^2 = 1/L_c$ ) leads to increased asymmetry of probabilities and so to the further increased PDG and parameter  $R$  (solid lines in Figs. 5 (a, c)).

PDG has a minimum as a function of noise power  $\sigma^2 = 1/L_c$  for amplitude and phase modulation (Fig. 5 (b)). When the birefringence fluctuations are large (small correlation lengths) and low (large correlation lengths) polarization pulling is dominating and PDG is high (Fig. 5 (b)). If fluctuations are large, escape events happen at very small intervals and so at larger intervals the fiber looks isotropic with small changes in pump and signal SOPs along the fiber. The case of small birefringence fluctuations corresponds to the polarization maintaining (PM) fiber where pump and signal SOPs initially oriented along the fast or slow axes preserve their orientations along the fiber. For an optimal level of noise above the activation threshold, random hops are synchronized with modulation frequency and so SR takes the form of de-correlation of SOPs (minimum in PDG) [17,18]. As follows from Fig. 3(a), PDG is almost independent of modulation frequency  $k_{lf}$  for amplitude modulation in the limit of high frequency modulation. It is likely that if the fiber spinning oscillates so fast that the system feels mainly the averaged spinning which can be small and not enough to activate de-correlation of SOPs [18]. As a result, with increasing modulation frequency polarization pulling occurs instead of SOPs de-correlation (thick dotted line in Fig. 5 (b)). As mentioned before, low-frequency phase-modulation of fiber spinning can result in a DL phenomenon in the form of either polarization pulling or de-correlated SOPs depending on the phase. This results herein in a minimum in PDG as a function of correlation length (thin lines in Figs. 5 (b)). Parameter  $R$  can have maxima and minima as a function of a noise power  $\sigma^2 = 1/L_c$  and modulation frequency  $k_{lf}$  and so it is likely that our case corresponds to more complex cases of SR and DL. PMD parameter has maxima and minima as function of  $k_{lf}$  and  $L_c^{-1}$  which can be an indication of SR and DL presence for polarization properties of fiber described by Eqs. (14).

Thus, application of fast (2.7 m period) and slow (200-600 m period) amplitude or phase-modulated fiber spinning can result in activated polarization pulling or de-correlation of pump and signal SOPs. De-correlation is accompanied with simultaneous suppression of PDG and PMD to the 1.2 dB and 0.035 ps/km<sup>1/2</sup> respectively.

#### 4. Conclusion

In conclusion, we have developed an advanced vector model of a fiber Raman amplifier accounting for fiber spinning and random birefringence. Based on this model and the PMD model previously developed in [9], we characterize a Raman amplifier in terms of PDG, gain fluctuations and PMD. Unlike previous approaches, we demonstrated that it is possible simultaneously to de-correlate pump and signal SOPs and to suppress PDG and PMD. This new technique is based on application of fiber spinning with two different scales: fast spinning with period of 2.7 m and slow spinning with period of 200 – 6000 m for 10 km of single mode fiber. In view of the similarity of a two-scale periodically spun fiber Raman amplifier to a periodically driven excitable system, we have found resonance-like de-correlation of pump and signal SOPs and polarization pulling equivalent to the Stochastic Resonance and Dynamic Localization in excitable systems [17–19]. As a result, we demonstrate that it is possible to provide de-correlation of pump and signal SOPs and simultaneously suppress PDG and PMD to the 1.2 dB and 0.035 ps/km<sup>1/2</sup> respectively. The

practical implementation of the obtained results can be in the design of fiber Raman amplifier-based quasi-isotropic spatially and spectrally transparent media for high-speed fiber optic communication [20,21].

#### **Acknowledgment**

S. Sergeyev acknowledges financial support from the European Union program FP7 PEOPLE-2009-IEF (grant 253297).